materials

MDPI

Article

Improving Ammonia Detecting Performance of Polyaniline Decorated rGO Composite Membrane with GO Doping

Yubin Yuan [1,2], Haiyang Wu [1,2], Xiangrui Bu [1,2], Qiang Wu [1,2], Xuming Wang [1,2], Chuanyu Han [1,2], Xin Li [1,2,3], Xiaoli Wang [1,2,4] and Weihua Liu [1,2,5,*]

1 School of Microelectronics, School of Electronics and Information Engineering, Xi'an Jiaotong University, Xi'an 710049, China; yuan8262xy@stu.xjtu.edu.cn (Y.Y.); wuhaiyang@stu.xjtu.edu.cn (H.W.); bxr1212@stu.xjtu.edu.cn (X.B.); w18801757@163.com (Q.W.); xmwang_zw@126.com (X.W.); hanchuanyu@mail.xjtu.edu.cn (C.H.); lx@mail.xjtu.edu.cn (X.L.); xlwang@mail.xjtu.edu.cn (X.W.)
2 The Key Lab of Micro-nano Electronics and System Integration of Xi'an City, Xi'an 710049, China
3 Guangdong Shunde Xi'an Jiaotong University Academy, Xi'an Jiaotong University, NO.3 Deshengdong Road, Daliang, Shunde District, Foshan 528300, China
4 School of Science, Xi'an Jiaotong University, Xi'an 710049, China
5 Research Institute of Xi'an Jiaotong University, Hangzhou 311215, China
* Correspondence: lwhua@mail.xjtu.edu.cn; Tel.: +86-29-8266-3343

Abstract: Gas-sensing performance of graphene-based material has been investigated widely in recent years. Polyaniline (PANI) has been reported as an effective method to improve ammonia gas sensors' response. A gas sensor based on a composite of rGO film and protic acid doped polyaniline (PA-PANI) with GO doping is reported in this work. GO mainly provides NH_3 adsorption sites, and PA-PANI is responsible for charge transfer during the gas-sensing response process. The experimental results indicate that the NH_3 gas response of rGO is enhanced significantly by decorating with PA-PANI. Moreover, a small amount of GO mixed with PA-PANI is beneficial to increase the gas response, which showed an improvement of 262.5% at 25 ppm comparing to no GO mixing in PA-PANI.

Keywords: gas sensor; nanocomposites; reduced graphene oxide; graphene oxide; PA-PANI; protic acid doping; composite membrane

Citation: Yuan, Y.; Wu, H.; Bu, X.; Wu, Q.; Wang, X.; Han, C.; Li, X.; Wang, X.; Liu, W. Improving Ammonia Detecting Performance of Polyaniline Decorated rGO Composite Membrane with GO Doping. *Materials* **2021**, *14*, 2829. https://doi.org/10.3390/ma14112829

Academic Editor: Dusan Losic

Received: 13 April 2021
Accepted: 19 May 2021
Published: 25 May 2021

1. Introduction

Since the 21st century, information technology has become a prominent feature of human society's development and progress. In order to realize the interconnection of everything, various sensors with different layout types in production and life are needed as information acquisition terminals. Traditionally, gas sensors have been more applied in many aspects of industrial, medical, and environmental protection. With the development of Internet of Things (IoT) technology, gas sensors will penetrate many scenes of life: food production and safety [1,2], human health status detection [3,4], and home environment [5,6], etc. Due to the requirements of high accuracy, miniaturization, and low power consumption for gas sensors in the IoT application, micro gas sensors with integration convenience demonstrated prominent potential for further study [7,8]. Compared to traditional metal oxide gas sensors, sensors based on 2-dimensional semiconductor materials do not have to rely on a high-temperature working environment, which shows the prospect of low-energy and application in portable Internet of Things devices. As the first 2D semiconductor material prepared in the laboratory, graphene is a planar allotrope of carbon. All carbon atoms in graphene are connected in the form of covalent bonds in a single plane [9]. This is because, in graphene, the 2s orbitals of carbon atoms form sp_2 hybrid orbitals with $2p_x$ and $2p_y$ orbitals. Thus, carbon atoms can bond to each other tightly through σ-bands, which have the electrons localization property to generate the

morphology of plane connecting carbon atoms [9,10]. Therefore, graphene has large specific surface areas for gas molecule adsorption. Besides, $2p_z$ electrons form the weakly bounded π-bands to increase electrons transport on the surface of graphene, leading to excellent electrical properties and low current noise. These basic characteristics indicate that graphene-based two-dimensional materials show great potential in gas-sensing applications [11]. However, because of lacking dangling bonds on the surface, molecular adsorption is usually formed through Van der Waals interaction, which leads to limited gas adsorption capacity and selectivity of intrinsic graphene [12]. Thus, researchers tended to make some decorations on graphene to get a composite film. Decoration options like metal nanoparticles such as Pd [13], Pt [14], and Ag [15] and metal oxides like SnO_2 [16], PdO [17], and Cu_2O [18], etc. all presented the enhancement of gas-sensing performance, especially selectivity of graphene-based gas sensor.

Another possible choice is synthesizing functionalized graphene, like graphene oxide(GO) and reduced graphene oxide(rGO) [19–21]. Compared to intrinsic graphene, GO and rGO have a certain amount of groups such as carboxyl, hydroxyl, and epoxy on their surface [22]. As these functional groups could provide adsorption sites for gas molecules, GO and rGO have demonstrated their great potential for gas detecting. Recently, we have synthesized an oxygen plasma-treated CVD graphene/intrinsic graphene composite membrane for gas sensing [23]. The composite film reported in that work exhibited a fast response and recovery process, combining with high sensitivity. However, note that with many functional groups on its surface, GO inevitably shows poor conductivity as a characteristic of oxidation state [24,25]. In most cases, poor conductivity usually leads to high current noise in gas detecting. Moreover, after exposure in gas environments for a long time, dangling bonds on the surface of GO would be partially removed, which changes the character of GO and decreases the long-term stability [26]. When treating GO with reducing agents, oxygen-containing groups are removed extensively, which can increase conductance and long-term stability [27]. Further, if the time of reducing action is controlled precisely, we can get partially reduced GO, which reserves a fraction of surface groups. Partially reduced GO balances the property of electric conductivity and gas molecular adsorption capability.

Meanwhile, conductive polymers, such as polyaniline (PANI), have excellent gas sensitivity, acceptable conductivity, and excellent stability [28]. Polyaniline has been widely investigated and used because of its simple synthesis process, good chemical stability, and environmental friendliness. When treating with protic acid, PANI could gain proton from protic acid and form N^+-H bonds to increase charge transport property. Thus, PANI has H^+ transport on its molecular link, which usually demonstrates p-type doping [29,30]. Based on the conductive mechanism mentioned above, gas molecules, especially reducing gases, could deliver electrons to PANI and form de-doping, which gives another possible gas detection choice. Inspired by those basic theories, in this work, we use rGO instead of graphene as a conductive channel, and a layer of protic acid doped polyaniline (PA-PANI) is loaded on its top surface for ammonia detection. The composite film shows good ammonia detection performance. More importantly, when a small amount of GO is mixed in PA-PANI, the response is significantly improved by 262.5% to 25 ppm ammonia. The double-layer composite sensitive membrane also delivered the potential of gate tunable gas sensitivity for further study.

2. Materials and Methods

2.1. Sensor Fabrication

The schematic of the device fabrication process is depicted in Figure 1. The preparation method of PA-PANI is shown as follows. Firstly, 0.5 g polyaniline (98% purified, purchased from Cool Chemical Technology Co., Ltd., Beijing, China) was mixed with 50 mL hydrochloric acid (36–38%, purchased from China National Pharmaceutical Group Co., Ltd., Shanghai, China) after diluting the hydrochloric acid to pH = 1. The mixed suspension was treated with ultrasound to synthesize PA-PANI. Secondly, the synthesized suspen-

sion was centrifuged with DI water until the washing solution reached pH = 7, followed by centrifuged with ethanol twice. Thirdly, 0.15 g PA-PANI was dissolved in 30 mL N, *N*-Dimethylformamide (DMF) (≥99.5%, purchased from China National Pharmaceutical Group Co., Ltd., Shanghai, China) to form 5 mg/mL PA-PANI solution, which was mixed with 1.2 mg/mL GO (purchased from XFNANO Materials Technology Co., Ltd., Nanjing, China) dispersion subsequently to get different mass ratios of PA-PANI and GO among 30:0.5, 30:1, 30:1.5, and 30:2. The synthesis of rGO films also proceeded simultaneously. Firstly, the silicon substrate was cut into small cube pieces in order to fit the size of the interdigital electrode (IDE). The IDEs were fabricated on Al_2O_3 substrate with a size of 10 mm × 5 mm × 0.635 mm. There were seven pairs of Au electrodes with a width of 200 μm and a spacing of 200 μm on the substrate. Then, polymethyl methacrylate (PMMA, purchased from Micro Chem, Westborough, MA, USA) and GO dispersion were successively spin-coated on the silicon wafer and dried. Secondly, the Si/PMMA/GO structure was immersed in acetone to remove PMMA. After the complete GO film was "lift-off" from the silicon substrate and then transferred into 10 mg/mL L(+)- ascorbic acid (AR, purchased from China National Pharmaceutical Group Co., Ltd., Shanghai, China) solution for reducing treatment. In the end, the mixed PA-PANI and GO solution was drop-coasted onto the rGO surface, which had already been transferred onto the interdigital electrode (IDEs). The sensor's fabrication was finished after drying. Polyaniline before and after protic acid treating are shown in Figure S1.

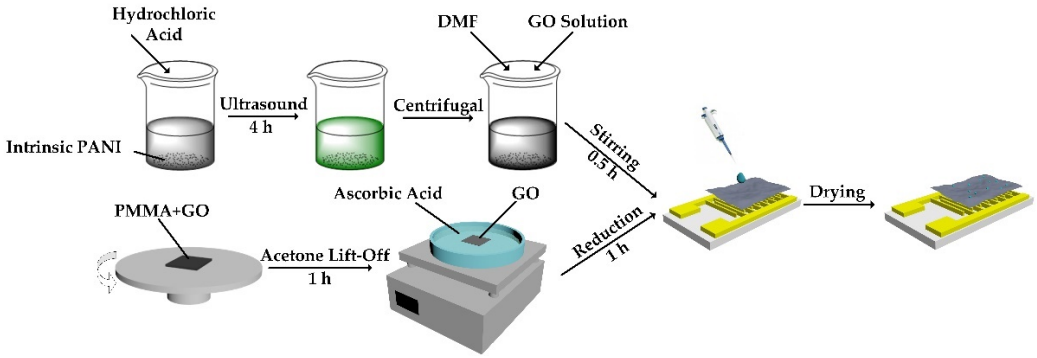

Figure 1. The schematic of the device fabrication process.

2.2. Measurement Setup

Figure 2 is a schematic diagram of the gas-sensing test system. The sensor was placed in an acrylic chamber with a volume of 4.67 L. The two ports of the chamber were connected to a pump to make sure the air current circulation in the sealed environment during testing. The concentration of NH_3 was controlled by the volume of gas injected through a syringe into the testing system. After the gas-sensing test, we opened the chamber and blew the test gas away with air. The response of the device was measured with a digital multimeter (Keithley 2000, Tektronix, Cleveland, OH, USA) and the data were read through LabVIEW on a laptop. Keithley 2000 implements resistance measurement by applying a constant current to the device and sampling the voltage. All the sensors worked at room temperature throughout the measurement.

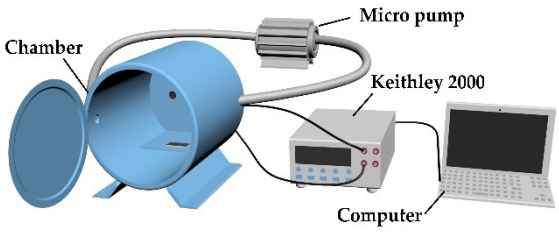

Figure 2. Schematic diagram of the gas-sensing test system.

2.3. Characterization Techniques

Field emission scanning electron microscopy (FESEM, GeminiSEM 500, Zeiss, Jena, Germany) was used to investigate the morphology of prepared samples. X-ray photoelectron spectroscopy (XPS, ESCALAB Xi+, Thermo Fisher Scientific, Waltham, MA, USA) analysis was performed to investigate the elemental composition of the samples of polyaniline, GO, and rGO. ESCALAB Xi+ has an Al/Mg double anode target X-ray source. When the energy scanning range is 0–1500 eV, the minimum scanning step size is 6 meV for the elemental composition analysis. The analysis area of ESCALAB Xi+ is 20 μm–8 mm.

3. Results

3.1. Material Characteristics

Field emission scanning electron microscopy (FE-SEM) was used for material characterization, and the results are displayed in Figure 3a–d. Figure 3a is the FE-SEM image of GO+PA-PANI/rGO composite sensitive membrane synthesized in the work for ammonia detection. The center of Figure 3a displays the cluster structure of PA-PANI and the irregular flocculent PA-PANI polymer with about 100 nm diameter could be seen when the image is enlarged as shown in Figure 3c. The background of Figure 3a shows rGO film which indicates good integrity and flatness. Most areas of rGO are very clean and flat, however, a small part has some wrinkles. Figure 3b indicates the good interaction property of GO and PA-PANI. Morphology of GO is displayed in Figure 3d, which is a magnification form of the lower right corner of Figure 3b.

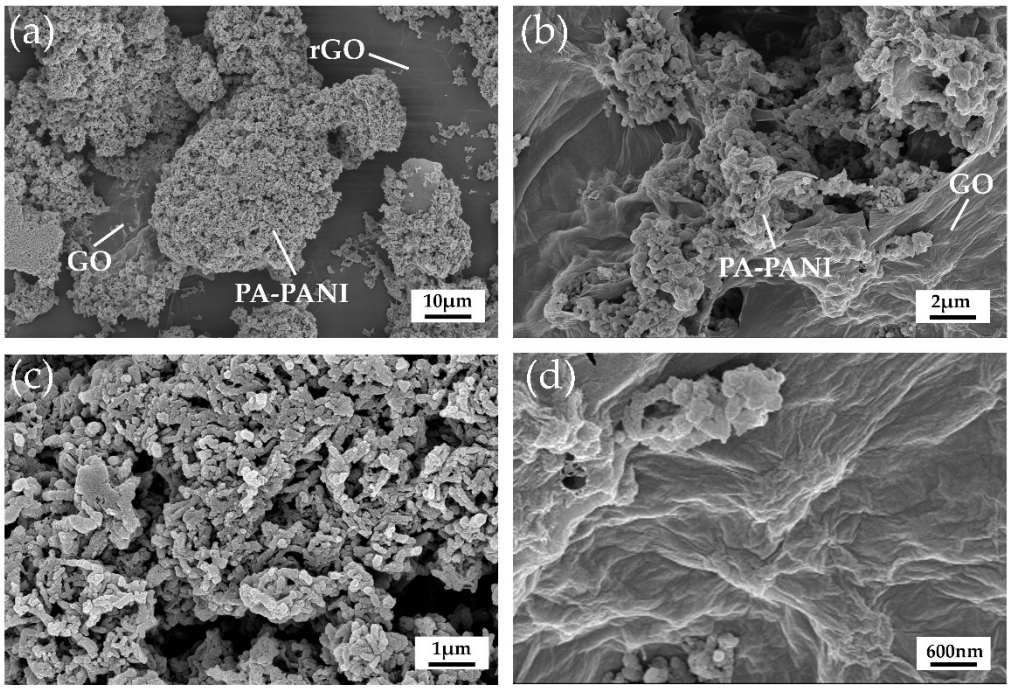

Figure 3. Characterization of materials by scanning electron microscopy. (**a**) The FE-SEM image of GO+PA-PANI/rGO composite sensitive membrane. (**b**) The FE-SEM image of PA-PANI and GO mixture. (**c**) The FE-SEM image of PA-PANI from (**a**). (**d**) The FE-SEM image of GO from (**b**).

This experiment also carried out X-ray photoelectron spectroscopy (XPS) analysis to characterize the elemental composition of polyaniline before and after proton acid doping. Figure 4a illustrates the spectra of PANI and PA-PANI, which has C1s peak at 285 eV, N1s peak at 399.96 eV, O1s peak at 532.2 eV [31,32]. Compared to PANI, PA-PANI has 7.13% chlorine atomic additionally at 198.2 eV. The appearance of Cl 2p peak can significantly improve that PANI was successfully doped by hydrochloric acid. Besides, N1s peak of PA-PANI are analyzed to verify that plenty of N atoms are successfully

protonated. The N1s peak of PA-PANI can be split into three peaks at the binding energy of 398.1, 399.4, and 401.6 eV [33], which correspond to =N-, -NH-, and -N+-, respectively. Among them, -N+- is the protonated part of N atoms which occupies 4.7%. In addition, XPS spectroscopy can also provide information about the element valence and bonding of GO and rGO. As p-electrons from the sp_2 carbon determine the optical and electrical properties of graphene-related materials in most cases, the analysis of sp_2 bonding can give us insight into the properties and structures of materials [34,35]. Thus, the C1s XPS spectrums of GO and rGO indicate the considerable content of oxidation groups on their surface. Therefore, in this work, to investigate detailed information of the chemical bonds in GO and rGO, the C1s peak at 285.72 eV are analyzed by AVANTAGE and the results are shown in Figure 4c,d. As shown in Table 1, C1s peaks of GO are split into four peaks at binding energy of 284.60, 286.90, 288.31, and 289 eV, which correspond to C-C=C, C-O, C=O, and O=C-O, and each of them occupies 49.72%, 45.14%, 3.24%, and 1.9% of the atomic content, respectively [36–38]. Nevertheless, for the atomic content in rGO, O=C-O and C=O disappear from the spectrogram completely while C–O has a sharp decrease to 22.51% and C-C=C increases to 77.49%. These results indicate the GO was partially reduced to rGO in L(+)- ascorbic acid solution.

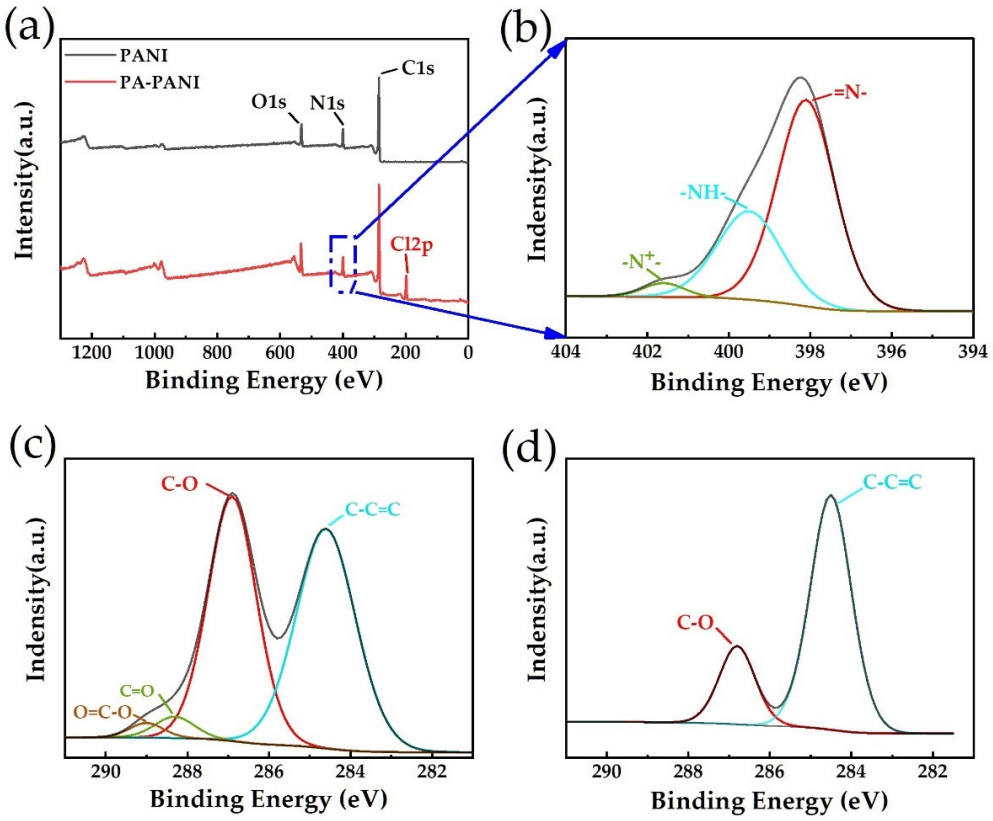

Figure 4. Characterization of materials by X-ray photoelectron spectroscopy. (**a**) XPS survey spectra of PA-PANI and PANI. (**b**) Zoom-in and fitting plot of PA-PANI's N1s peak in XPS spectra. (**c**) Zoom-in plot and fittings of GO's C1s peak in XPS spectra. (**d**) Zoom-in plot and fittings of rGO's C1s peak in XPS spectra.

Table 1. XPS analysis of C1s peak of GO and rGO.

Bands	GO	rGO
C-C=C (284.60 eV)	49.72%	77.49%
C-O (286.90 eV)	45.14%	22.51%
C=O (288.31 eV)	3.24%	none
O=C-O (289 eV)	1.9%	none

3.2. Gas-Sensing Experiment

The original resistance of the composite film with different PA-PANI/ GO's mixing ratio ranges from 3.7 K–5.6 KΩ. The sensitivity test obtains the change in the resistance of the sensors. In order to deliver clear and visualized data to make comparisons, the corresponding relative responses of the sensors to NH_3 are discussed in the following paragraphs. Further, the sensor's response can be defined as Equation (1):

$$\text{Response} = [(R - R_0)/R_0] \times 100\%, \quad (1)$$

where R_0 is the original resistance of the composite sensitive membrane before injecting NH_3 gas, and R is the real-time resistance of the composite sensitive membrane during the NH_3 sensing experiment.

We firstly made up rGO and PA-PANI/ rGO composite membrane comparison groups to explore the phenomenon of ammonia sensing enhancement property with PA-PANI loading. As shown in Figure 5a, the sensitive membrane with only rGO reduced by L(+)- ascorbic acid solution merely gives response at 15.2% to 200 ppm ammonia, which mainly resulted from residual oxygen-containing groups on the surface of rGO that were substantiated by XPS spectra in Figure 4d. Nevertheless, rGO decorated with PA-PANI has a much more prominent response as shown in Figure 5b. Compared to pure rGO, rGO decorated with PA-PANI has a maximum enhancement of 50.2% to 200 ppm NH_3. In previous literature reports, polyaniline doped by hydrochloric acid demonstrated p-type electrical conductivity [39]. At the same time, it is worth noting that NH_3 is a kind of reducing gases, which tend to give electronics to other sensitive materials. Thus, consistent with the conclusions shown in Figure 5, PA-PANI is an ideal material for ammonia detection. Besides, when response time is accurately controlled to 3 min every testing cycle, it can clearly be obtained from the curves in Figure 5 that the sensor with only the rGO membrane does not appear to have any tendency to saturate. However, the response of the PA-PANI/ rGO composite membrane has already tended to saturate, and this phenomenon seems much obvious to 150, 100, 50, and 25 ppm NH_3, especially. The result indicated the faster response to NH_3 for the PA-PANI/ rGO composite membrane. Moreover, the recovery curve for the pure rGO membrane shows a lousy roughness characteristic, combined with a longer recovery time. By contract, the PA-PANI/ rGO composite membrane provides a rough recovery curve with low noise and a decline of recovery time at 48% compared to pure rGO on average.

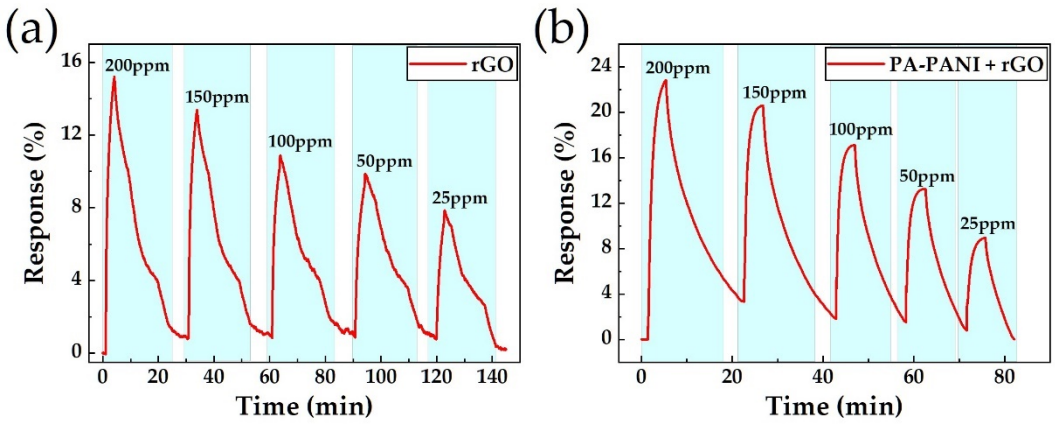

Figure 5. The relative NH_3 gas-sensing test results. (**a**) Test results of pure rGO membrane-based sensors. (**b**) PA-PANI/rGO composite membrane-based sensors.

Further, in order to improve gas sensitivity, we tend to make some decorations in PA-PANI. Some first-principles calculations have already proved that the appropriate introduction of defects and doping can enhance the sensitivity of graphene-based gas

sensors [40,41]. Thus, GO seems to be a good choice, as it brings plenty of organic functionalizations to the surface and is quite easy for synthesizing in the laboratory. It is worth considering that carboxyl usually displays the character of hydrogen-bonding acidity, which both apt to incorporate with amido from PA-PANI and show advances in NH_3 adsorption. Therefore, we mixed PA-PANI with GO to bring molecular adsorbed sites. In this work, we made different mixing ratios of PA-PANI and GO at 30:0.5, 30:1, 30:1.5, and 30:2. The results of gas-sensing response are displayed in Figure 6a–d and the linear fitting of gas-response for different mix proportions are shown in Figure 6e.

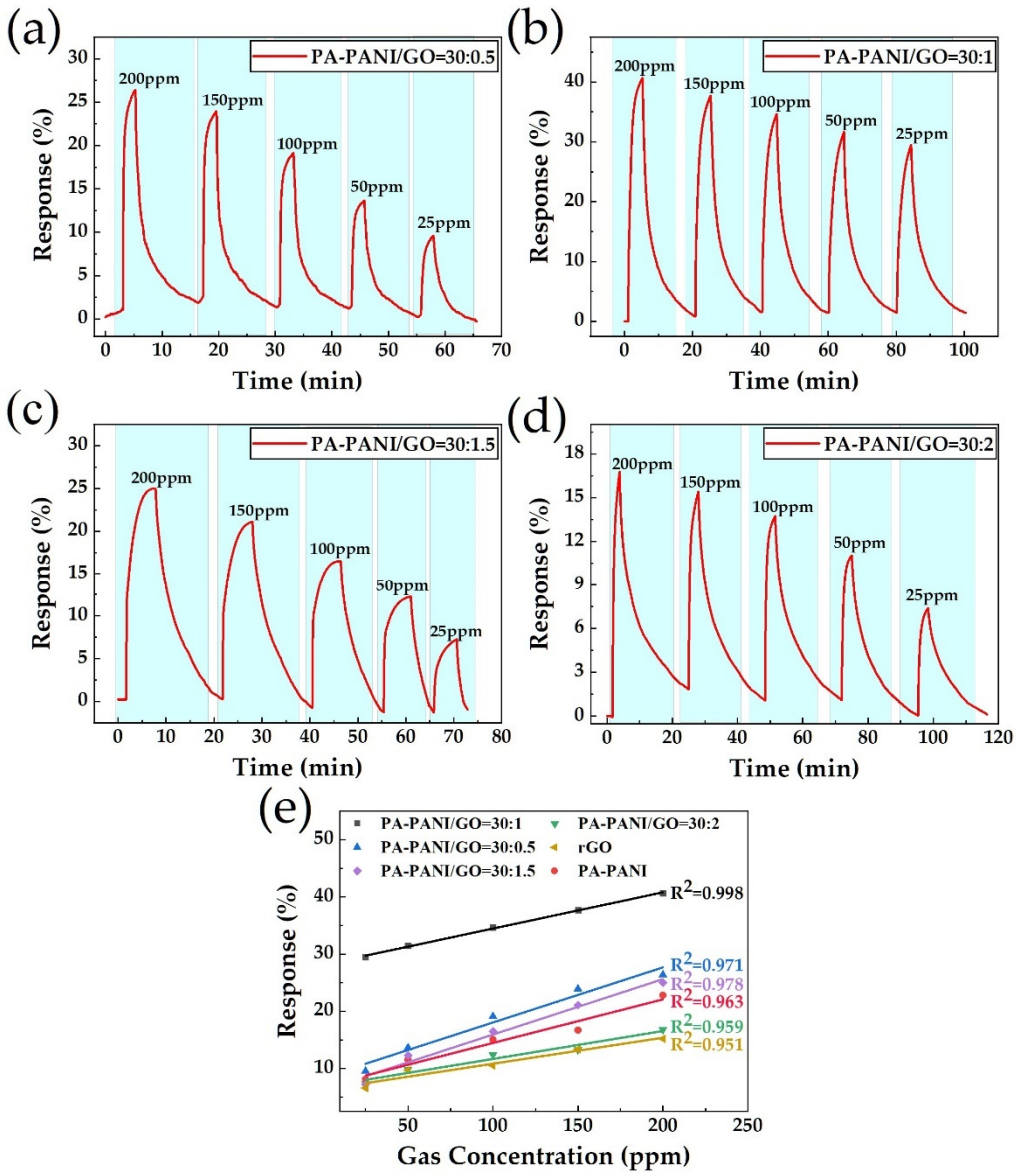

Figure 6. Gas-sensing response based on mixing ratio of (**a**) 30:1 PA-PANI and GO; (**b**) 30:1.5 PA-PANI and GO; (**c**) 30:0.5 PA-PANI and GO; (**d**) 30:2 PA-PANI and GO; (**e**) Linear regression of response for different mix proportions of every group.

As shown in the response curves displayed above, when mixing PA-PANI with a little bit of GO, the response is further improved. Especially to the situation of 30:1 mixing ratio, as shown in Figure 6a, the responsivity to 200 and 25 ppm NH_3 reaches 40.56% and 29.46%, respectively. The optimal relative response improvement achieves 262.5% to 25 ppm and 78% to 200 ppm compared to the result of nothing mixed with PA-PANI shown in Figure 5b, which indicates that a little bit of GO doping in PA-PANI as decoration

material would significantly enhance the NH_3 gas-sensing behavior. The result is attributed to the functionalized groups, which provided molecular grippers and adsorption sites for NH_3, on GO. Besides, from the linear fitting of gas-response for different decoration proportions, it is obvious that the group of 30:1 mixing ratio also has the best regression coefficient at 0.998. However, due to the lack of electrical conductivity, too much GO dose in the decoration material will block the possible charge transfer path and result in a degradation of the gas-sensing performance.

3.3. Mechanism Analysis

The chemical process of PA-PANI synthesizing and the possible mechanism for gas-sensing improvement are shown in Figure 7. When doped with protic acid, the number of electrons does not change. In the doping process, H^+ firstly protonates the nitrogen atom on the imine, which makes the valence band of the doping segment on the polyaniline chain appear with holes, that is, P-type doping, forming a stable delocalized form of poly (emerald-imine) atomic group. The positive charge of the imine nitrogen atom is dispersed to adjacent atoms along the molecular chain through conjugation, which improves the stability of the entire molecular chain [42]. The effect of an external electric field, through the resonance of the conjugated electrons, causes the hole to move along the entire chain, showing electrical conductivity.

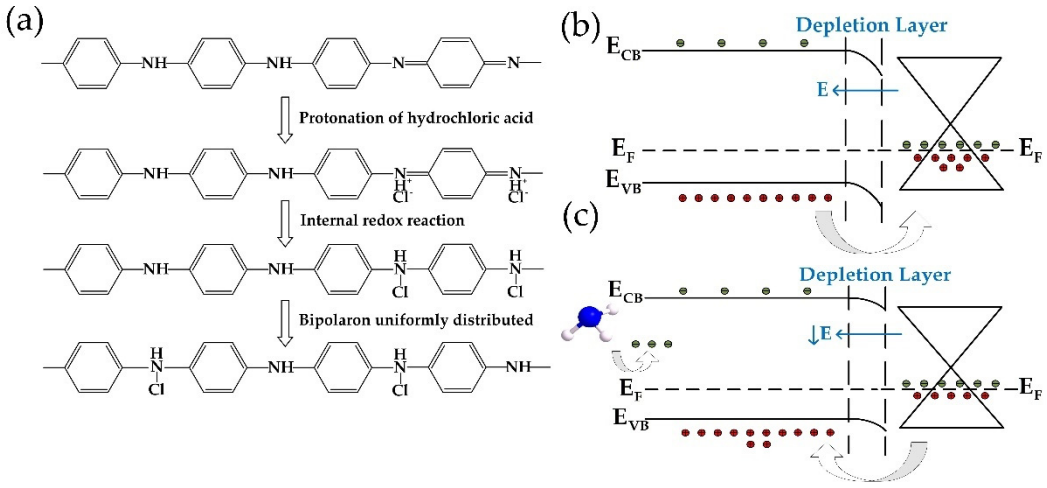

Figure 7. (**a**) Process of hydrochloric acid doping intrinsic PANI. (**b**) Schematic of the junction between PA-PANI and rGO. (**c**) Schematic of charge transport through the junction between PA-PANI and rGO when NH_3 is adsorbed.

As rGO is primarily made up of honeycomb hexagonal rings of carbon atoms, while PA-PANI also has plenty of benzene rings on its molecular links, rGO and PA-PANI have some similarities in material structures. Based on semiconductor heterojunction theory, materials with similar crystal structures and atomic spacing can form a heterojunction at the contact interface. Because rGO was slightly reduced in the ascorbic acid (as indicated in Figure 3d) and polyaniline was heavily doped by hydrochloric acid, rGO synthesized in this work has fewer carriers and lower conductivity. Therefore, when PA-PANI and rGO contact, a hole diffuses from PA-PANI to rGO and leads to the formation of a depletion layer and a built-in electric field from rGO to PA-PANI as shown in Figure 7b. As a result, PA-PANI and rGO form a p-p$^-$ junction. When the junction forms, as a kind of reducing gas, ammonia can be considered as a donor when chemical adsorption occurs on the surface of the sensitive membrane, and the amount of gas adsorbed is mainly enhanced by GO doping. When NH_3 provides electrons to the PA-PANI, electron concentration inside the PA-PANI increases. The electrons brought by NH_3 reduce the doping level of PA-PANI, and further decrease the built-in electric field at the interaction of rGO and PA-PANI. Therefore, some of the hole in rGO would flow back to PA-PANI, which decreases the hole

concentration in rGO, as indicated in Figure 7c. The final result of the carrier concentration decreasing inside rGO is consistent with the gas-sensitive response data of resistance increase. Note that due to its chain rigidity and strong chain interaction, PA-PANI has poor solubility and is almost insoluble in most common organic solvents, even in strongly polar liquid like DMF. Moreover, the amount of PA-PANI dripping on the rGO surface is tightly controlled during sensor fabrication. So, the morphology of PA-PANI decorated on rGO's surface demonstrates the character of clusters instead of the continuous thin film. Thus, the resistance of the composite membrane is mainly provided by rGO which is directly connected to IDEs. Based on the mechanism mentioned above, the resistance of the composite membrane would increase during gas detecting, which is consistent with the experimental results.

4. Conclusions

In conclusion, a composite sensitive membrane of a PA-PANI/GO mixture decorated rGO was synthesized and tested as a gas-sensing material. When the mixing ratio of PANI and GO is 30:1, the highest improvement of NH_3 gas-sensing response achieves 262.5% at 25 ppm NH_3 compared to no GO decorating in PA-PANI. The improved gas-sensing performance can be explained as GO provides effective NH_3 adsorption sites while PA-PANI is responsible for the charge transmission. A reasonable charge transmission process is proposed: NH_3 brings N-type doping to PA-PANI and leads to hole transport from rGO to PA-PANI, which finally induces the gas-sensitive response. Such a gas-sensing mechanism enriches the strategy of composite gas-sensing material design.

Supplementary Materials: The following are available online at https://www.mdpi.com/article/10.3390/ma14112829/s1, Figure S1: The figures for polyaniline before and after protic acid treating, Figure S2: The response curve of the repeatability test for membrane with the mixture ratio of 30:1 in 25 ppm NH_3.

Author Contributions: Conceptualization, Y.Y. and X.B.; methodology, Y.Y., H.W. and Q.W.; validation, W.L.; formal analysis, Y.Y. and X.B.; investigation, Y.Y., H.W. and X.W. (Xuming Wang); resources, X.W. (Xiaoli Wang), X.L. and C.H.; data curation, Y.Y.; writing—original draft, Y.Y. and H.W.; writing—review and editing, Y.Y. and W.L.; supervision, W.L.; funding acquisition, W.L., X.W. (Xiaoli Wang), X.L. and C.H. All authors have read and agreed to the published version of the manuscript.

Funding: This research was financially supported by the National Natural Science Foundation of China (Grant Nos. 61671368, 61704137 and 91123018); Basic Public Welfare Research Planning Project of Zhejiang Province (LGG19F040002); Science and Technology Planning Project of Guangdong Province, China (2017A010103004), and the Fundamental Research Funds for the Central Universities.

Institutional Review Board Statement: Not applicable.

Informed Consent Statement: Not applicable.

Data Availability Statement: Not applicable.

Acknowledgments: The material analysis work was done at Instrument Analysis Center of Xi'an Jiaotong University.

Conflicts of Interest: The authors declare no conflict of interest.

References

1. Wei, Z.B.; Wang, J.; Jin, W.F. Evaluation of varieties of set yogurts and their physical properties using a voltammetric electronic tongue based on various potential waveforms. *Sens. Actuators B Chem.* **2013**, *177*, 684–694. [CrossRef]
2. Chang, L.Y.; Chuang, M.Y.; Zan, H.W.; Meng, H.F.; Lu, C.J.; Yeh, P.H.; Chen, J.N. One-Minute Fish Freshness Evaluation by Testing the Volatile Amine Gas with an Ultrasensitive Porous-Electrode-Capped Organic Gas Sensor System. *ACS Sens.* **2017**, *2*, 531–539. [CrossRef] [PubMed]
3. Nasiri, N.; Clarke, C. Nanostructured Gas Sensors for Medical and Health Applications: Low to High Dimensional Materials. *Biosensors* **2019**, *9*, 43. [CrossRef] [PubMed]

4. Righettoni, M.; Amann, A.; Pratsinis, S.E. Breath analysis by nanostructured metal oxides as chemo-resistive gas sensors. *Mater. Today* **2015**, *18*, 163–171. [CrossRef]
5. Jung, Y. Hybrid-Aware Model for Senior Wellness Service in Smart Home. *Sensors* **2017**, *17*, 1182. [CrossRef]
6. Ghayvat, H.; Mukhopadhyay, S.; Gui, X.; Suryadevara, N. WSN- and IOT-Based Smart Homes and Their Extension to Smart Buildings. *Sensors* **2015**, *15*, 10350–10379. [CrossRef] [PubMed]
7. Arafat, M.M.; Dinan, B.; Akbar, S.A.; Haseeb, A.S. Gas sensors based on one dimensional nanostructured metal-oxides: A review. *Sensors* **2012**, *12*, 7207–7258. [CrossRef] [PubMed]
8. Zhang, J.; Qin, Z.; Zeng, D.; Xie, C. Metal-oxide-semiconductor based gas sensors: Screening, preparation, and integration. *Phys. Chem. Chem. Phys.* **2017**, *19*, 6313–6329. [CrossRef] [PubMed]
9. Novoselov, K.S.; Geim, A.K.; Morozov, S.V.; Jiang, D.; Zhang, Y.; Dubonos, S.V.; Grigorieva, I.V.; Firsov, A.A. Electric Field Effect in Atomically Thin Carbon Films. *Science* **2004**, *306*, 666–669. [CrossRef] [PubMed]
10. Geim, A.K.; Novoselov, K.S. The rise of graphene. *Nat. Mater.* **2007**, *6*, 183–191. [CrossRef]
11. Yang, S.X.; Jiang, C.B.; Wei, S.H. Gas sensing in 2D materials. *Appl. Phys. Rev.* **2017**, *4*, 021304–021338. [CrossRef]
12. Dan, Y.; Lu, Y.; Kybert, N.J.; Luo, Z.; Johnson, A.T. Intrinsic response of graphene vapor sensors. *Nano. Lett.* **2009**, *9*, 1472–1475. [CrossRef] [PubMed]
13. Pak, Y.; Kim, S.M.; Jeong, H.; Kang, C.G.; Park, J.S.; Song, H.; Lee, R.; Myoung, N.; Lee, B.H.; Seo, S.; et al. Palladium-Decorated Hydrogen-Gas Sensors Using Periodically Aligned Graphene Nanoribbons. *ACS Appl. Mater. Inter.* **2014**, *6*, 13293–13298. [CrossRef] [PubMed]
14. Rad, A.S.; Abedini, E. Chemisorption of NO on Pt-decorated graphene as modified nanostructure media: A first principles study. *Appl. Surf. Sci.* **2016**, *360*, 1041–1046. [CrossRef]
15. Ghanbari, R.; Safaiee, R.; Sheikhi, M.H.; Golshan, M.M.; Horastani, Z.K. Graphene Decorated with Silver Nanoparticles as a Low Temperature Methane Gas Sensor. *ACS Appl. Mater. Int.* **2019**, *11*, 21795–21806. [CrossRef]
16. Hu, J.C.; Chen, M.P.; Rong, Q.; Zhang, Y.M.; Wang, H.P.; Zhang, D.M.; Zhao, X.B.; Zhou, S.Q.; Zi, B.Y.; Zhao, J.H.; et al. Formaldehyde sensing performance of reduced graphene oxide-wrapped hollow SnO_2 nanospheres composites. *Sens. Actuators B Chem.* **2020**, *307*, 127584. [CrossRef]
17. Arora, K.; Srivastava, S.; Solanki, P.R.; Puri, N.K. Electrochemical Hydrogen Gas Sensing Employing Palladium Oxide/Reduced Graphene Oxide (PdO-rGO) Nanocomposites. *IEEE Sens. J.* **2019**, *19*, 8262–8271. [CrossRef]
18. Zhou, L.S.; Shen, F.P.; Tian, X.K.; Wang, D.H.; Zhang, T.; Chen, W. Stable Cu_2O nanocrystals grown on functionalized graphene sheets and room temperature H2S gas sensing with ultrahigh sensitivity. *Nanoscale* **2013**, *5*, 1564–1569. [CrossRef]
19. Wang, T.; Huang, D.; Yang, Z.; Xu, S.; He, G.; Li, X.; Hu, N.; Yin, G.; He, D.; Zhang, L. A Review on Graphene-Based Gas/Vapor Sensors with Unique Properties and Potential Applications. *Nano-Micro Lett.* **2016**, *8*, 95–119. [CrossRef]
20. Chen, W.; Deng, F.F.; Xu, M.; Wang, J.; Wei, Z.B.; Wang, Y.W. GO/Cu_2O nanocomposite based QCM gas sensor for trimethylamine detection under low concentrations. *Sens. Actuators B Chem.* **2018**, *273*, 498–504. [CrossRef]
21. Abideen, Z.U.; Kim, J.-H.; Mirzaei, A.; Kim, H.W.; Kim, S.S. Sensing behavior to ppm-level gases and synergistic sensing mechanism in metal-functionalized rGO-loaded ZnO nanofibers. *Sens. Actuators B Chem.* **2018**, *255*, 1884–1896. [CrossRef]
22. Krishnamoorthy, K.; Veerapandian, M.; Yun, K.; Kim, S.J. The chemical and structural analysis of graphene oxide with different degrees of oxidation. *Carbon* **2013**, *53*, 38–49. [CrossRef]
23. Wu, H.; Bu, X.; Deng, M.; Chen, G.; Zhang, G.; Li, X.; Wang, X.; Liu, W. A Gas Sensing Channel Composited with Pristine and Oxygen Plasma-Treated Graphene. *Sensors* **2019**, *19*, 625. [CrossRef] [PubMed]
24. Yu, X.; Cheng, H.; Zhang, M.; Zhao, Y.; Qu, L.; Shi, G. Graphene-based smart materials. *Nat. Rev. Mater.* **2017**, *2*, 1–13. [CrossRef]
25. Tan, C.; Cao, X.; Wu, X.J.; He, Q.; Yang, J.; Zhang, X.; Chen, J.; Zhao, W.; Han, S.; Nam, G.H.; et al. Recent Advances in Ultrathin Two-Dimensional Nanomaterials. *Chem. Rev.* **2017**, *117*, 6225–6331. [CrossRef]
26. Kim, S.; Zhou, S.; Hu, Y.; Acik, M.; Chabal, Y.J.; Berger, C.; de Heer, W.; Bongiorno, A.; Riedo, E. Room-temperature metastability of multilayer graphene oxide films. *Nat. Mater.* **2012**, *11*, 544–549. [CrossRef]
27. Becerril, H.A.; Mao, J.; Liu, Z.; Stoltenberg, R.M.; Bao, Z.; Chen, Y. Evaluation of solution-processed reduced graphene oxide films as transparent conductors. *Acs Nano* **2008**, *2*, 463–470. [CrossRef]
28. Li, D.; Huang, J.X.; Kaner, R.B. Polyaniline Nanofibers: A Unique Polymer Nanostructure for Versatile Applications. *Acc. Chem Res.* **2009**, *42*, 135–145. [CrossRef]
29. Kang, E.T.; Neoh, K.G.; Tan, K.L. Polyaniline: A polymer with many interesting intrinsic redox states. *Prog. Polym. Sci.* **1998**, *23*, 277–324. [CrossRef]
30. Baker, C.O.; Huang, X.; Nelson, W.; Kaner, R.B. Polyaniline nanofibers: Broadening applications for conducting polymers. *Chem. Soc. Rev.* **2017**, *46*, 1510–1525. [CrossRef]
31. Wang, Y.; Gao, X.; Zhang, L.J.; Wu, X.M.; Wang, Q.G.; Luo, C.Y.; Wu, G.L. Synthesis of Ti_3C_2/Fe_3O_4/PANI hierarchical architecture composite as an efficient wide-band electromagnetic absorber. *Appl. Surf. Sci.* **2019**, *480*, 830–838. [CrossRef]
32. Sedighi, A.; Montazer, M.; Mazinani, S. Synthesis of wearable and flexible NiP0.1-SnOx/PANI/CuO/cotton towards a non-enzymatic glucose sensor. *Biosens. Bioelectron.* **2019**, *135*, 192–199. [CrossRef] [PubMed]
33. Kang, E.T.; Neoh, K.G.; Tan, K.L. Esca Studies of Protonation in Polyaniline. *Polym. J.* **1989**, *21*, 873–881. [CrossRef]
34. Pei, S.; Cheng, H.-M. The reduction of graphene oxide. *Carbon* **2012**, *50*, 3210–3228. [CrossRef]

35. Robertson, J.; O'Reilly, E.P. Electronic and atomic structure of amorphous carbon. *Phys. Rev. B* **1987**, *35*, 2946–2957. [CrossRef] [PubMed]
36. Chen, W.F.; Yan, L.F. Preparation of graphene by a low-temperature thermal reduction at atmosphere pressure. *Nanoscale* **2010**, *2*, 559–563. [CrossRef] [PubMed]
37. Zhang, Z.H.; Zhang, J.W.; Cao, C.F.; Guo, K.Y.; Zhao, L.; Zhang, G.D.; Gao, J.F.; Tang, L.C. Temperature-responsive resistance sensitivity controlled by L-ascorbic acid and silane co-functionalization in flame-retardant GO network for efficient fire early-warning response. *Chem. Eng. J.* **2020**, *386*, 123894. [CrossRef]
38. Zhan, Y.H.; Wang, J.; Zhang, K.Y.; Li, Y.C.; Meng, Y.Y.; Yan, N.; Wei, W.K.; Peng, F.B.; Xia, H.S. Fabrication of a flexible electromagnetic interference shielding Fe_3O_4@ reduced graphene oxide/natural rubber composite with segregated network. *Chem. Eng. J.* **2018**, *344*, 184–193. [CrossRef]
39. Tohidi, S.; Parhizkar, M.; Bidadi, H.; Mohamad-Rezaei, R. High-performance chemiresistor-type NH3 gas sensor based on three-dimensional reduced graphene oxide/polyaniline hybrid. *Nanotechnology* **2020**, *31*, 415501. [CrossRef]
40. Zhang, Y.H.; Chen, Y.B.; Zhou, K.G.; Liu, C.H.; Zeng, J.; Zhang, H.L.; Peng, Y. Improving gas sensing properties of graphene by introducing dopants and defects: A first-principles study. *Nanotechnology* **2009**, *20*, 185504. [CrossRef]
41. Boukhvalov, D.W.; Dreyer, D.R.; Bielawski, C.W.; Son, Y.W. A Computational Investigation of the Catalytic Properties of Graphene Oxide: Exploring Mechanisms by using DFT Methods. *ChemCatChem* **2012**, *4*, 1844–1849. [CrossRef]
42. Chiang, C.K.; Fincher, C.R.; Park, Y.W.; Heeger, A.J.; Shirakawa, H.; Louis, E.J.; Gau, S.C.; MacDiarmid, A.G. Electrical Conductivity in Doped Polyacetylene. *Phys. Rev. Lett.* **1978**, *40*, 1472. [CrossRef]